

Finite element analysis of RC tension member based on pseudo-discrete crack model

F.J. Ma¹⁾, *P.L. Ng²⁾ and A.K.H. Kwan³⁾

^{1), 2), 3)} *Department of Civil Engineering, The University of Hong Kong, Hong Kong SAR, China*

²⁾ *Faculty of Civil Engineering, Vilnius Gediminas Technical University, Vilnius LT-10223, Lithuania*

²⁾ irdngpl@gmail.com

ABSTRACT

Conventionally, crack analysis of reinforced concrete (RC) members may be conducted by using the finite element method based on smeared crack model or discrete crack model. However, both the smeared and discrete representations of cracks have their own deficiencies. The smear crack model could not realistically reflect the crack paths and hence could not compute crack widths correctly. Whilst the discrete crack model is difficult to apply because of the need to adaptively generate discrete crack elements according to the cracks formed during the loading process. By transforming and reformulating the smeared crack model, a pseudo-discrete crack model is developed for finite element implementation. Moreover, the novel crack queuing algorithm is introduced to simulate the stress redistribution during cracking. The analysis method allows accurate computation of the crack spacing, widths and pattern. To verify its applicability and accuracy, the method is applied to analyse RC tension members in the literature, whereby satisfactory numerical results are obtained. Furthermore, the cracking behaviour of tension members reinforced with high-strength steel bars is studied.

1. INTRODUCTION

Conventionally, crack analysis of reinforced concrete (RC) members may be conducted by using the finite element method based on smeared crack model or discrete crack model. The smeared crack model assumes that the whole concrete element is cracked (Rots and Blaauwendraad 1989; Ohmenhäuser et al. 1998), i.e. the crack formed could be smeared over the concrete element as proposed by Rashid

¹⁾ PhD Student

²⁾ Researcher

³⁾ Professor

(1968). The analysis process is relatively straightforward and thus many existing finite element programmes are based on the smeared crack model. However, although the tensile strain across the cracks in the cracked element can be evaluated, since the tensile strain across a crack is actually dependent on the gauge length (Bazant and Oh 1983), the crack width cannot be determined from the tensile strain. Therefore, the smeared crack model does not enable the determination of crack widths.

The smeared crack model may be further categorized into the non-rotating crack model and rotating crack model (Ohmenhäuser et al. 1998). The former assumes the crack directions to be fixed once the cracks are formed (Rashid 1968). The fixed crack direction represents the material axis of orthotropy. In general, shear stress may arise if the principal axes rotate. The latter allows the cracks to rotate with the principal strain directions (De Borst and Nauta 1985). As such, no shear stress would arise across the crack surfaces. Comparatively, the non-rotating crack model can more realistically reflect the orientation of cracks, while both models could not trace the crack paths due to the smearing of cracks in a continuous fashion.

The discrete crack model requires the cracks to follow element edges (Rots and Blaauwendraad 1989). In order to achieve this, simplifying assumptions had been made to either pre-determine the crack location (Ngo and Scordelis 1967), or restrict the cracks to follow the element boundaries (Nilson 1968). For better accuracy of analysis, adaptive re-meshing to allow for crack propagations during the loading process may be implemented (Yang and Chen 2005; Kanakubo et al. 2012). However, such adaptive re-meshing incurs rather complicated algorithms in the programming as well as great demands of computational resources, which has limited its applications.

Apart from cracks, the steel reinforcing bars may be modelled by the smeared bar approach or the discrete bar approach. The former smears the steel bars within the concrete elements (Gupta and Akbar 1984), whilst the latter models the steel bars by discrete bar elements (Jendele and Cervenka 2006). The discrete bar approach offers the main advantage of allowing for the bond slip of steel bars. This is done by inserting interface elements between the discrete bar elements and concrete elements. On the other hand, the smeared bar approach is not able to account for the bond slip.

By transforming and reformulating the smeared crack model, a pseudo-discrete crack model has recently been developed for finite element implementations (Ng et al. 2015). The model is able to circumvent the sophistication of altering the mesh topology by adaptive re-meshing and hence it is computationally efficient. The non-rotating crack model and discrete bar approach are adopted. Moreover, the novel crack queuing algorithm is introduced to simulate the stress redistribution during cracking, so as to accurately capture the crack patterns in RC structures. The analysis method can realistically reflect the cracking behaviour. Herein, the pseudo-discrete crack model is applied to the analysis of RC tension members.

2. PSEUDO-DISCRETE CRACK MODEL

2.1 Constitutive Modelling

The pseudo-discrete crack model was implemented in a nonlinear finite element programme developed by the authors. Details of the modelling strategies by the finite

element method have been reported elsewhere (Ng et al. 2015; Ma and Kwan 2015) and hence is not repeated in this paper. In the analysis, tension positive-compressive negative sign convention is adopted. To cater for the post-peak loading regime where the load-deformation response descends, direct iteration based on secant stiffness is performed throughout the solution process.

The concrete is modelled by 4-noded quadrilateral elements. The resistance of concrete is determined from the biaxial strength envelope by Kupfer and Gerstle (1973). The notion of equivalent uniaxial strain (Wang et al. 1999) is adopted to transform the biaxial stress-strain relations into uniaxial stress-strain relations. In an uniaxial direction, for concrete under compression, the stress-strain curve by Desayi and Krishnan (1964) is used; while for concrete under tension, linearly elastic behaviour up to cracking is assumed and the concrete is regarded to have no tensile resistance thereafter.

The reinforcing bars are modelled by one-dimensional 2-noded discrete bar elements. The stress-strain relation is taken to be linearly elastic and plastic with strain hardening (Mander 1983). The bond between concrete and reinforcing steel is modelled by 4-noded bond interface elements with infinitesimal thickness. The element topology is the same as that put forward by Goodman et al. (1968). The bond stress-slip relation in accordance with FIB Model Code 2010 (Fédération Internationale Du Béton 2013) is used. Among each of the two nodal pairs, one node is connected to concrete and the other is connected to reinforcing bar. The two nodes have the same coordinates but individual degrees of freedom. A discrete shear spring is employed to simulate the bond stiffness.

2.2 Integrated Concrete Cracking Criterion

Since the stress field at a crack tip is singular, the tensile stresses in the proximity of a crack tip would be extremely high, especially when a fine mesh is used. Hence, if the cracking criterion of concrete is based only on tensile strength, the cracks may propagate in an uncontrollable manner. To overcome such numerical difficulty, an integrated concrete cracking criterion combining tensile strength and fracture toughness has been proposed and the full derivation can be referenced from the relevant literature (Kwan et al. 1999, 2017; Ma and Kwan 2015). Basically, taking into account the stress intensity factor of concrete (Erdogan and Sih 1963; Chao and Liu 1997), the fracture toughness criterion for crack propagation is given by

$$\sigma_{\theta} \geq \frac{K_{IC}}{\sqrt{2\pi r}} \quad (1)$$

where σ_{θ} is the circumferential stress (the stress perpendicular to the line joining the point being considered to the crack tip), r is the distance from the point being considered to the crack tip, and K_{IC} is the fracture toughness.

The implementation of integrated concrete cracking criterion is as follows. For each element, the parameter r_o (the value of r where $K_{IC}/(2\pi r)^{0.5}$ is equal to the tensile strength) is determined. If there is no crack tip within a distance of r_o from the element centroid, the tensile strength criterion is used. Otherwise, the value of r is determined with respect to the closest crack tip, and the fracture toughness criterion is applied.

2.3 Crack Queuing Algorithm

In nonlinear analysis, the loading is applied in discrete increments and iterations are performed in each increment step. During iteration, every concrete element is judged one by one against the cracking criteria and suppose all concrete elements satisfying the cracking criteria are allowed to crack simultaneously. This would lead to erroneous crack pattern and is also against the reality because upon the formation of a crack, there would be stress redistribution and the tensile stress orthogonal to the crack would be relieved thereby eluding the formation of other cracks in close proximity. The stress redistribution has to be accounted for by re-analysing the element stresses before allowing other cracks to form. For this reason, the authors advocate the incorporation of crack queuing algorithm (Kwan et al. 1999; Ng et al. 2015) in crack analysis.

The implementation of the crack queuing algorithm is as follows. Within each iteration, if there is no concrete element satisfying the cracking criterion, no new crack is formed and the analysis can proceed to the next loading step. Otherwise, only the concrete element that surpasses the integrated cracking criterion to the greatest extent is allowed to crack, and its stiffness matrix is adjusted with the secant stiffness normal to the crack reduced to a very small value. The whole structure is then re-analysed at the same loading level so as to allow the stress redistribution to take place. This procedure is repeated until no element satisfies the integrated cracking criterion, and the analysis can proceed to the next loading step. With crack queuing algorithm employed, the resulting crack patterns would be more realistic compared to the smeared crack modelling.

2.4 Determination of Crack Width

A major advantage of the pseudo-discrete crack model is to assume the crack to be formed inside the concrete element and avoid re-meshing. The crack width is determined directly from the nodal displacements. As illustrated in Fig. 1, consider a crack passing through the centroid of quadrilateral concrete element. At each side of the crack, the node furthest from the crack is identified. Denote the node at right side furthest from the crack by node J, and the node at left side furthest from the crack by node L. The displacement of node J away from the crack d_J and the displacement of node L away from the crack d_L are given respectively by:

$$d_J = +u_J \cos \alpha + v_J \sin \alpha \quad (2)$$

$$d_L = -u_L \cos \alpha - v_L \sin \alpha \quad (3)$$

in which u_J and v_J are the displacements of node J in the x - and y -directions, u_L and v_L are the displacements of node L in the x - and y -directions, respectively, and α is the crack angle (angle between the normal to the crack and the x -axis). The crack width w is calculated as the sum of displacements of the two nodes away from the crack. A negative value of w means that the crack is under compression, and should be regarded as closed.

$$w = d_J + d_L \quad (4)$$

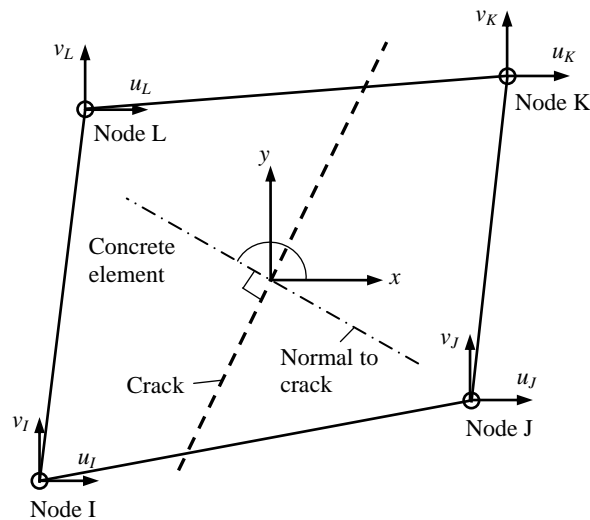


Fig. 1 Crack width determination

3. ANALYSIS OF RC TENSION MEMBERS

3.1 Details of Tension Members

RC tension members tested by Radnić and Markota (2003) and studied by Soltani et al. (2013) are analysed using the pseudo-discrete crack approach. The dimensions and structural configurations of the tension members are tabulated in Table 1. Three experimental specimens in Radnić and Markota (2003) numbered F8-RA, F10-RA and F12-RA are included in the analysis to verify the pseudo-discrete crack model against the cracking behavior observed from experiments. All the specimens have a cross-section of 70.0×70.0 mm and a length of 700 mm. In each specimen, only one steel reinforcing bar is embedded at the centre of the concrete section. The steel ratios (steel area to concrete area ratios) are 1.03%, 1.60% and 2.31%. The steel bars are deformed bars with yield strength of 400 MPa and ultimate strength of 500 MPa. The initial elastic modulus, tensile strain at start of strain hardening and ultimate tensile strain are taken as 200 GPa, 1.0% and 10.0%, respectively. The concrete has compressive strength of 24.1 MPa and tensile strength of 1.8 MPa. The initial elastic modulus, Poisson's ratio and fracture toughness are taken to be 23.2 GPa (calculated per American Standard ACI 318M-14), 0.2 and $1.3 \text{ MNm}^{-1.5}$ (calculated per suggestion by Chen et al. (2011)). The parameters of bond stress-slip relation are evaluated according to FIB Model Code 2010.

Twelve numerical specimens in Soltani et al. (2013) are analysed to examine the effects of high-strength steel bar configurations on the cracking behaviour. The specimens have different cross-sections as listed in Table 1. In each specimen, only one steel reinforcing bar is embedded at the centre of the concrete section. The steel bars are high-strength deformed bars. The yield strength and ultimate strength of bars with diameters 12.7 mm, 19.0 mm, 25.4 mm and 32.0 mm are (965, 1200), (841, 1110), (820, 1069) and (820, 1069) MPa. Three different steel ratios of 0.75%, 1.00% and 1.50% are considered for each bar size. The compressive strength, tensile strength and

initial elastic modulus of concrete are 34.5 MPa, 3.3 MPa and 27.8 GPa, respectively. The parameters of bond stress-slip relation are evaluated as per Model Code 2010.

Table 1 Dimensions and structural configurations of RC tension members

Member reference	Cross-section (mm)	Steel bar configuration	Steel ratio (%)
F8-RA	70.0×70.0	1 no. ϕ 8.0 mm	1.03
F10-RA	70.0×70.0	1 no. ϕ 10.0 mm	1.60
F12-RA	70.0×70.0	1 no. ϕ 12.0 mm	2.31
D4-0.75	130.0×130.0	1 no. ϕ 12.7 mm	0.75
D6-0.75	194.4×194.4	1 no. ϕ 19.0 mm	0.75
D8-0.75	259.9×259.9	1 no. ϕ 25.4 mm	0.75
D10-0.75	327.5×327.5	1 no. ϕ 32.0 mm	0.75
D4-1.00	112.6×112.6	1 no. ϕ 12.7 mm	1.00
D6-1.00	168.4×168.4	1 no. ϕ 19.0 mm	1.00
D8-1.00	225.1×225.1	1 no. ϕ 25.4 mm	1.00
D10-1.00	283.6×283.6	1 no. ϕ 32.0 mm	1.00
D4-1.50	91.9×91.9	1 no. ϕ 12.7 mm	1.50
D6-1.50	137.5×137.5	1 no. ϕ 19.0 mm	1.50
D8-1.50	183.8×183.8	1 no. ϕ 25.4 mm	1.50
D10-1.50	231.6×231.6	1 no. ϕ 32.0 mm	1.50

3.2 Results of Cracking Behaviour

For the tension members tested by Radnić and Markota (2003), the experimental and analytical maximum crack widths are plotted against the steel stress in Fig. 2 to Fig. 4. It can be seen that for specimen F8-RA (Fig. 2), the analytical and measured crack widths are approximately equal at steel stress of 140 MPa, thereafter the analytical crack width becomes larger than the measured result along with increasing steel stress, but when the steel stress is higher than 240 MPa, the discrepancy diminishes gradually to almost zero at a steel stress of 400 MPa. For specimen F10-RA (Fig. 3), the analytical and measured crack widths agree with each other at all steel stress levels with no larger than 7% error. For specimen F12-RA (Fig. 4), the analytical crack width is slightly larger than the measured result when the steel stress is lower than 250 MPa but slightly smaller than the measured result when the steel stress is higher than 250 MPa. Overall, the experimental and analytical crack widths of the specimens agree considerably well with each other.

To illustrate the computed crack patterns generated by the pseudo-discrete crack model, the crack patterns of specimen F12-RA at different loading stages are compared with the experimental results reported by Radnić and Markota (2013) and depicted in Fig. 5. When the applied tension force is equal to 11 kN, 4 cracks (1 is full-width while 3 are discontinuous) were observed experimentally while there is 1 crack in the analytical crack pattern. When the applied tension force is increased to 20 kN, 5 cracks (3 are full-width while 2 are discontinuous) were observed from the experimental crack pattern, while the analytical crack pattern contains 3 cracks. When the applied tension force is further increased to 30 kN, the experimental crack number was 7 (5 are full-width while 2 are discontinuous) whereas the analytical crack number is 6. Finally at

tension force of 40 kN, the experimental crack number became 12 (all are full-width) and the analytical crack number increases to 15.

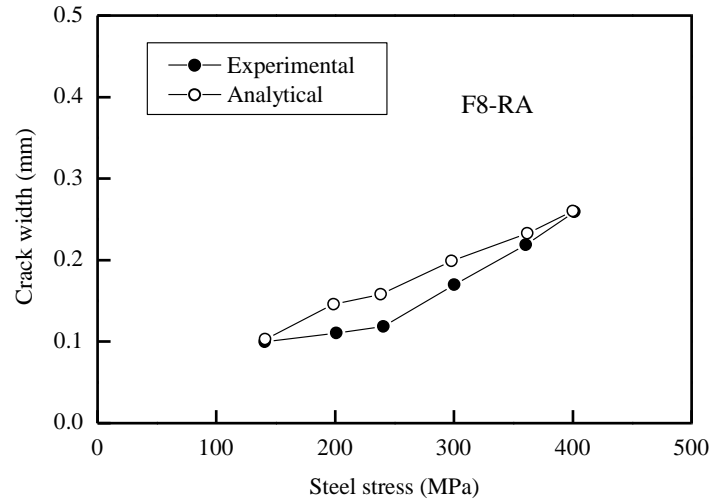


Fig. 2 Crack width of F8-RA

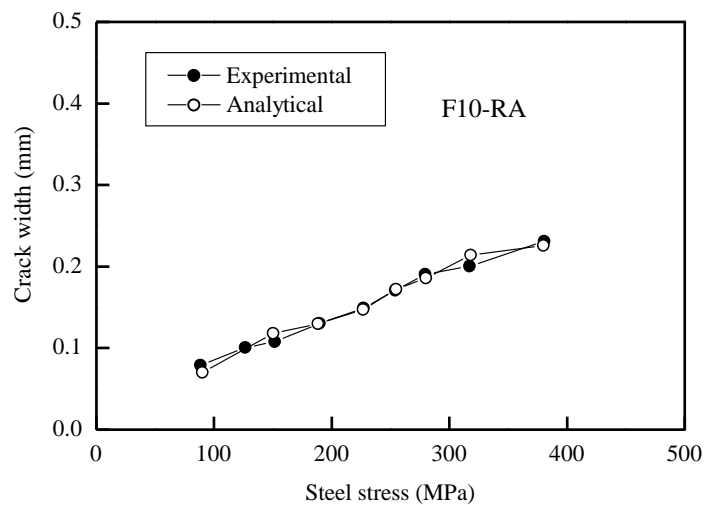


Fig. 3 Crack width of F10-RA

Overall speaking, the experimental crack pattern and spacing demonstrated certain degree of randomness, because the intrinsic random variations of material properties in reality would affect the locations of cracks. On the other hand, the analytical crack pattern and spacing are fairly regular, because the constitutive properties of materials are assumed to be uniform in the finite element analysis. Though this assumption could be replaced by stochastic variations of material properties, the experimental crack pattern may not be reproduced analytically due to the randomness factor. Nonetheless, the pseudo-discrete crack model combined with crack queuing algorithm is capable of producing crack patterns with clearly defined discrete cracks that are reasonably in line with the experimental results.

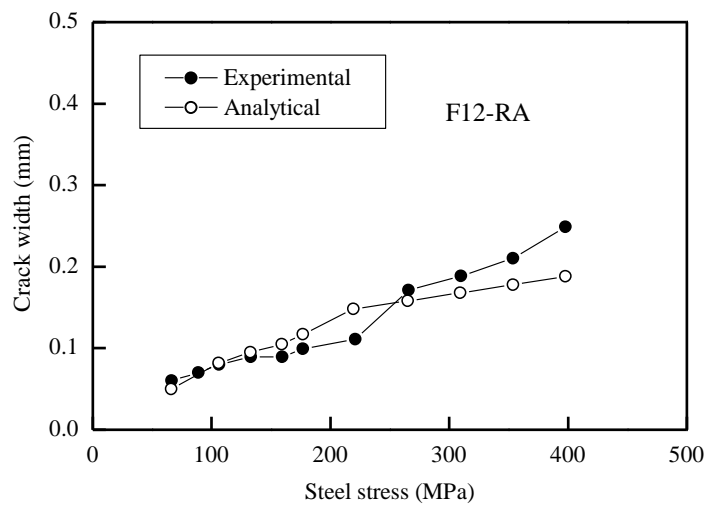


Fig. 4 Crack width of F12-RA

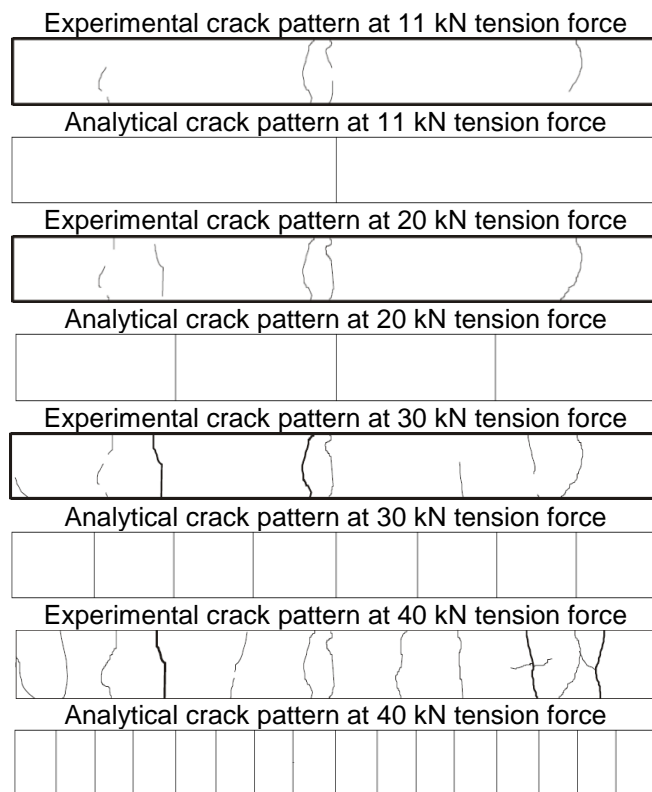


Fig. 5 Crack patterns of F12-RA

3.3 Effects of High-Strength Steel Bar Configurations

The use of high-strength reinforcing steel bars has been gaining popularity. Typically, high-strength steel bars have yield strength substantially higher than the conventional high-yield deformed bars, and can be in the range from 500 MPa to well above 800 MPa; while the elastic modulus of high-strength steel bars is similar to that of conventional steel reinforcing bars. Since the working stress of the high-strength

steel bars is usually higher, the steel strain induced is also higher and therefore the crack widths in the RC structure are likely to be larger. Such potentially larger crack widths may cause serviceability and durability problems, and should be properly dealt with in the design stage. On this aspect, systematic research on the cracking and deformation behaviour of concrete structures reinforced with high-strength steel bars is necessary, in order to develop a reliable methodology of estimating crack widths. Along this research direction, the effects of high-strength steel bar configurations including steel ratio and bar size are examined through analyses of the numerical RC tension specimens studied by Soltani et al. (2013) as listed in Table 1.

Using the pseudo-discrete crack model, the analytical crack widths of the specimens with different bar sizes and steel ratios are plotted against the steel stress, and are compared with the computed results of Soltani et al. (2013), as depicted in Fig. 6 to Fig. 8. The crack width of specimens with steel ratio fixed at 0.75% is shown in Fig. 6, from which it can be seen that for relatively large bar size (25.4 and 32.0 mm), the results of Soltani et al. and the authors are in good matching. At steel ratio of 1.00%, as seen in Fig. 7, for smaller bar sizes (12.7 and 19.0 mm), the crack widths are consistently underestimated in Soltani et al.; whereas for larger bar sizes (25.4 and 32.0 mm), the crack widths are underestimated in Soltani et al. at steel stresses smaller than 600 MPa but overestimated at steel stresses larger than 600 MPa. Fig. 8 plots the crack widths of specimens with steel ratio fixed at 1.50%, it is seen that the calculated crack widths for the specimen of 19.0 mm bar size are in good matching, but those for the specimens of other bar sizes are more discrepant.

All in all, the two sets of analysis results are in reasonably desirable agreement for the majority of specimens, with discrepancies possibly due to the different numerical methods used. However, it is important to note that the resulting crack widths would be too large. Consider the steel stress level of say 60% of the yield strength, it is seen from Fig. 6 to Fig. 8 that the corresponding crack widths are in the range from 0.3 mm to 0.9 mm, which are excessive from serviceability and durability points of view. At this juncture, both sets of analysis results reveal that: (1) the crack width generally increases with the steel stress; (2) at the same steel ratio, the crack width is larger when the bar size is larger; and (3) at the same bar size, the crack width is smaller when the steel ratio is higher. With respect to these phenomena, the authors recommend the following ways to reduce the crack width: To use a larger number of smaller diameter steel bars; and to keep the steel ratio sufficiently high. In this regard, further research is needed to develop more specific design guidelines.

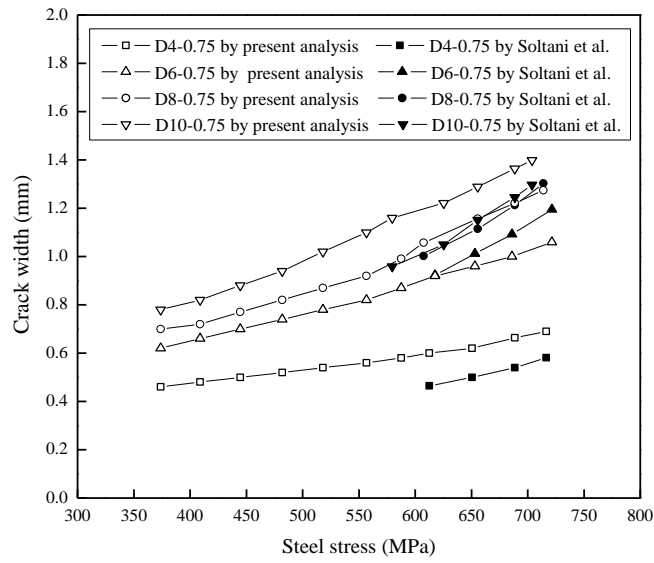


Fig. 6 Crack widths at steel ratio of 0.75%

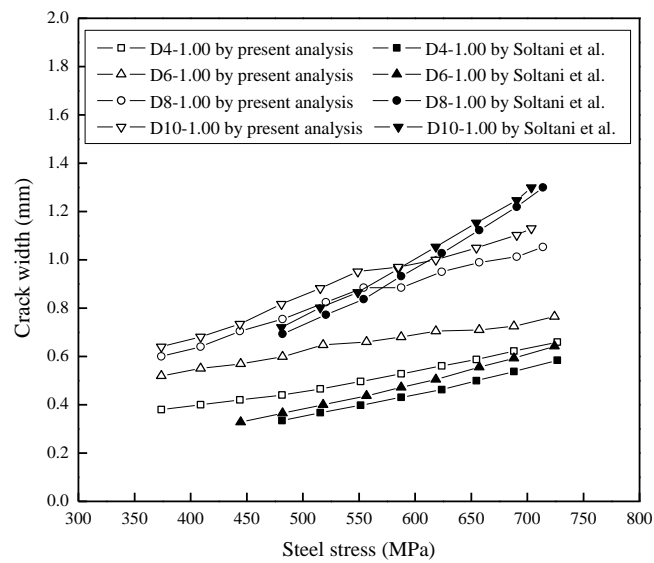


Fig. 7 Crack widths at steel ratio of 1.00%

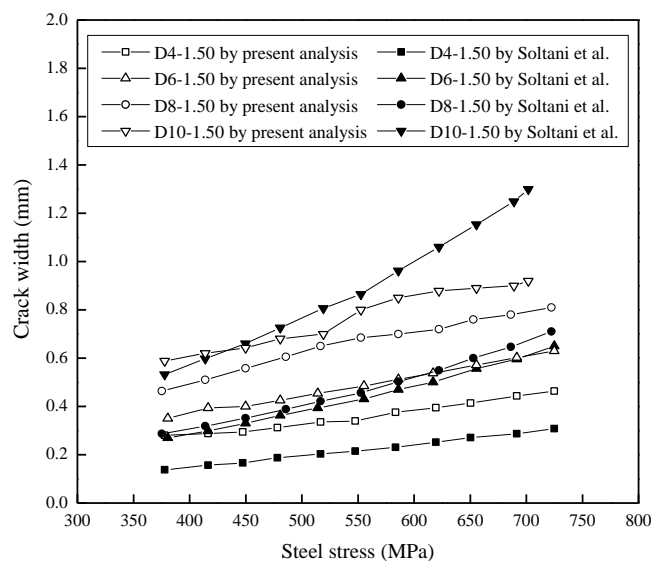


Fig. 8 Crack widths at steel ratio of 1.50%

4. CONCLUSIONS

The pseudo-discrete crack model for nonlinear finite element analysis of reinforced concrete (RC) structures has been developed, with the incorporation of integrated concrete cracking criterion to tackle the singularity at crack tips, crack queuing algorithm to cater for the stress redistribution upon formation of new crack, and method to determine crack width from the nodal displacements of concrete element. RC tension members in the literature have been analysed to verify the model. The analytical results have demonstrated desirable agreement with experimental results. In addition, the pseudo-discrete crack model has been applied to the analysis of tension members reinforced with high-strength steel bars. Based on the results, the authors recommend that crack width should be reduced by using a larger number of smaller diameter steel bars and keeping the steel ratio sufficiently high.

ACKNOWLEDGEMENTS

The support by Marie Skłodowska-Curie Actions of the European Commission (Project No. 751461) is gratefully acknowledged.

REFERENCES

- Bažant, Z.P. and Oh, B.H. (1983), "Crack band theory for fracture of concrete", *Materials and Structures*, **16**(3), 155-177.
- Chao, Y.J. and Liu, S. (1997), "On the failure of cracks under mixed-mode loads", *International Journal of Fracture*, **87**(3), 201-223.

- Chen, H.H., Su, R.K.L. and Kwan, A.K.H. (2011), "Fracture toughness of plain concrete made of crushed granite aggregate", *Transactions, Hong Kong Institution of Engineers*, **18**(2), 6-12.
- De Borst, R. and Nauta, P. (1985), "Non-orthogonal cracks in a smeared finite element model", *Engineering Computations*, **2**(1), 35-46.
- Desayi, P. and Krishnan, S. (1964), "Equation for the stress-strain curve of concrete", *ACI Journal*, **61**(3), 345-350.
- Erdogan, F. and Sih, G.C. (1963), "On the crack extension in plates under plane loading and transverse shear", *Journal of Basic Engineering, ASME*, **85**(4), 519-525.
- Fédération Internationale Du Béton (2013), fib Model Code for Concrete Structures 2010, Ernst & Sohn, Berlin, Germany.
- Goodman, R.E., Taylor, R.L. and Brekke, T.L. (1968), "A model for the mechanics of jointed rock", *Journal of Soil Mechanics and Foundation Division, ASCE*, **94**(3), 637-659.
- Gupta, A.K. and Akbar, H. (1984), "Cracking in reinforced concrete analysis", *Journal of Structural Engineering, ASCE*, **110**(8), 1735-1746.
- Jendele, L. and Cervenka, J. (2006), "Finite element modelling of reinforcement with bond", *Computers and Structures*, **84**(28), 1780-1791.
- Kanakubo, T., Sato Y., Uchida Y., Watanabe K. and Shima H. (2012), "Japan Concrete Institute TC activities on bond behavior and constitutive laws in RC (Part 3 Application of constitutive laws for FEA)", In: Proceedings of Bond in Concrete 2012, 105-112.
- Kupfer, H.B. and Gerstle, K.H. (1973), "Behavior of concrete under biaxial stresses", *Journal of Engineering Mechanics Division, ASCE*, **99**(4), 853-866.
- Kwan, A.K.H., Wang, Z.M. and Chan H.C. (1999), "Mesoscopic study of concrete II: nonlinear finite element analysis", *Computers and Structures*, **70**(5), 545-556.
- Kwan, A.K.H., Ng, P.L. and Wang, Z.M. (2017), "Mesoscopic analysis of crack propagation in concrete by nonlinear finite element method with crack queuing algorithm", *Procedia Engineering*, **172**, 620-627.
- Ma, F.J. and Kwan, A.K.H. (2015), "Crack width analysis of reinforced concrete members under flexure by finite element method and crack queuing algorithm", *Engineering Structures*, **105**, 209-219.
- Mander, J.B. (1983), Seismic Design of Bridge Piers, PhD Thesis, University of Canterbury, New Zealand.
- Ng, P.L., Ma, F.J. and Kwan, A.K.H. (2015), "Crack analysis of concrete beams based on pseudo-discrete crack model", In: D. Fernando, J.G. Teng & J.L. Torero (eds), Proceedings of the Second International Conference on Performance-based and Life-cycle Structural Engineering, Brisbane, Australia, 669-678.
- Ngo, D. and Scordelis, A.C. (1967), "Finite element analysis of reinforced concrete beams", *ACI Journal*, **64**(3), 152-163.
- Nilson, A.H. (1968), "Nonlinear analysis of reinforced concrete by the finite element method", *ACI Journal*, **65**(9), 757-766.
- Ohmenhäuser, F., Weihe, S. and Kröplin B. (1998), "Classification and algorithmic implementation of smeared crack models", In: R. de Borst, N. Bićanić, H.A. Mang & G. Meschke (eds), Proceedings, Euro-C 1998: Computational Modelling of Concrete Structures, Badgastein, Austria, 173-182.

- Radnić, J. and Markota, L. (2003), "Experimental verification of engineering procedures for calculation of crack width in concrete elements", *International Journal for Engineering Modelling*, **16**(1), 63-69.
- Rashid, Y.R. (1968), "Ultimate strength analysis of prestressed concrete pressure vessels", *Nuclear Engineering and Design*, **7**(4), 334-344.
- Rots, J.G. and Blaauwendraad, J. (1989), "Crack models for concrete: discrete or smeared? fixed, multi-directional or rotating?", *Heron*, **34**(1), 1-59.
- Soltani, A., Harries, K.A. and Shahrooz, B.M. (2013), "Crack opening behavior of concrete reinforced with high strength reinforcing steel", *International Journal of Concrete Structures and Materials*, **7**(4), 253-264.
- Wang, Z.M., Kwan, A.K.H. and Chan, H.C. (1999), "Mesoscopic study of concrete I: generation of random aggregate structure and finite element mesh", *Computers and Structures*, **70**(5), 533-544.
- Yang, Z.J. and Chen, J.F. (2005), "Finite element modelling of multiple cohesive discrete crack propagation in reinforced concrete beams", *Engineering Fracture Mechanics*, **72**(14), 2280-2297.